Direct measurement of Bacon-Shor code stabilizers

Muyuan Li, Daniel Miller, and Kenneth R. Brown

Phys. Rev. A **98**, 050301 — Published 6 November 2018

DOI: 10.1103/PhysRevA.98.050301

Direct measurement of Bacon-Shor code stabilizers

Muyuan Li,[1] Daniel Miller,[2] and Kenneth R. Brown[1,3,*]

[1] *School of Computational Science and Engineering, Georgia Institute of Technology, Atlanta, Georgia 30332, USA*

[2] *Institut für Theoretische Physik III, Heinrich-Heine-Universität Düsseldorf, D-40225 Düsseldorf, Germany*

[3] *Departments of Electrical and Computer Engineering, Chemistry, and Physics, Duke University, Durham, NC 27708, USA*

A Bacon-Shor code is a subsystem quantum error-correcting code on an $L \times L$ lattice where the $2(L-1)$ weight-$2L$ stabilizers are usually inferred from the measurements of $2L(L-1)$ weight-2 gauge operators. Here we show that the stabilizers can be measured directly and fault tolerantly with bare ancillary qubits by constructing circuits that follow the pattern of gauge operators. We then examine the implications of this method for small quantum error-correcting codes by comparing distance 3 versions of the rotated surface code and the Bacon-Shor code with the standard depolarizing model and in the context of a trapped ion quantum computer. We find that for a simple circuit of prepare, error correct and measure the Bacon-Shor code outperforms the surface code by requiring fewer qubits, taking less time, and having a lower error rate.

Quantum information experiments are approaching the number of qubits and operational fidelity necessary for quantum error correction to improve performance [1–3]. Classical error correction on quantum devices have already shown the ability to suppress introduced errors and increase memory times [4–8]. Two promising quantum error-correcting codes for data qubits arranged on an $L \times L$ lattice are the surface code [9–11] and the Bacon-Shor code [12–14]. Numerical simulation of the surface code shows a high memory threshold of 1% error per operation for increasing L and for distance 3 codes a pseudothreshold of 0.3% error per operation for a depolarizing error model [11]. The Bacon-Shor code is a subsystem code and has no threshold as L grows [15] but promising performance for small distance codes with a pseudothreshold of 0.2% for a depolarizing error model [14] and a fault-tolerant protocol for implementing universal gates without distillation [16]. The rotated surface code has L^2-1 check operators with $(L-1)^2$ checks of weight 4 in the bulk and $2(L-1)$ checks of weight 2 on the boundary [10]. The advantage of the Bacon-Shor code comes from using $2L(L-1)$ weight-2 gauge operators to determine the weight-$2L$ check operators and the lack of threshold is a result of having only $2(L-1)$ checks [12, 14, 15].

In this Letter, we first describe the relationship between the Bacon-Shor and surface codes with the compass model. We then use the gauge operators defined by the compass model to generate circuits that fault-tolerantly measure the weight-$2L$ Bacon-Shor stabilizers and the weight-4 surface code stabilizers using bare ancillary qubits. We then compare state preparation for the $L \times L$ Bacon-Shor and surface codes. Finally, we examine how these general results lead to a practical advantage for the Bacon-Shor code over the surface code on a 3×3 lattice under a generic error model and a more specific ion trap error model.

In condensed matter physics the compass model is used to describe a family of lattice models involving interacting quantum degrees of freedom [17]. The relationship between compass model and topological quantum computing is also well-studied, e.g, Kitaev's honeycomb model [18]. Fig. 1a shows a 9-qubit compass model on a square lattice. Subsystem error-correcting codes arise naturally from the compass model, where the interactions between neighboring qubits can be viewed as weight-2 gauge operators [12]. The compass model also has a 90° rotation symmetry, so that X and Z Pauli errors are treated symmetrically. Examining Fig. 1 we see that the stabilizer generators of the rotated surface code and the Bacon-Shor code can be considered as different constraints on the parity of products of gauge operators. This process of choosing constraints is referred to as gauge fixing. For the surface code, each weight-2 stabilizer is exactly a gauge operator of the corresponding type, and each weight-4 stabilizer is equivalent to fixing the parity of the product of two gauge operators on the same face; for the Bacon-Shor code, each weight-L stabilizer is equivalent to fixing the parity of the product of L gauge operators in the same double row or column of qubits.

A challenge for constructing fault-tolerant syndrome measurement circuits is the propagation of errors from the ancillary qubits used for measurement to the data qubits that hold the information. This type of error is commonly referred to as a hook error, a generalization of the definition in Ref. [19]. A k-fault-tolerant procedure yields the correct result if k or less errors happen. For a quantum error correcting code of distance d, the code is $\lfloor d/2 \rfloor$-fault-tolerant to single qubit errors when syndrome measurements are perfect. In order to maintain a $\lfloor d/2 \rfloor$-fault-tolerant procedure for noisy syndrome circuits, the syndromes must be measured multiple times and the measurement circuit must not generate uncontrolled errors on data qubits. The original approach of fault-tolerant syndrome measurement uses verified multi-

* ken.brown@duke.edu

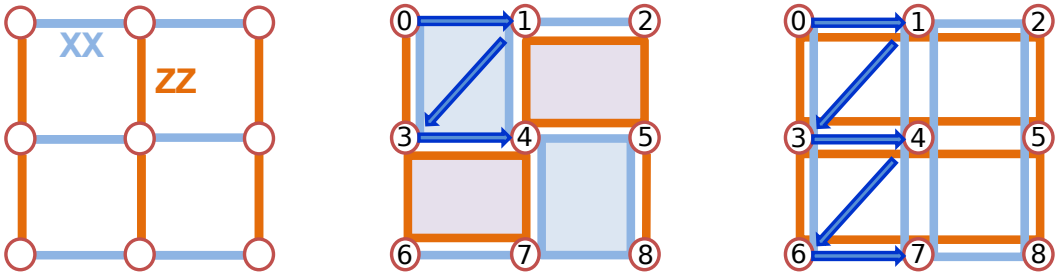

(a) Compass Model (b) Surface (c) Bacon-Shor

FIG. 1: The compass model with ZZ bonds along the vertical axis and XX bonds along the horizontal axis. Choices of gauge on a 3×3 lattice lead to two well-known stabilizer codes: [[9,1,3]] surface code and [[9,1,3]] Bacon-Shor code . The underlying bonds of the compass model are a guide for how to fault tolerantly measure surface code and Bacon-Shor code stabilizers with bare ancillary qubits. Measuring stabilizers in order of gauge operators can help suppress hook errors on two-qubit gates in the stabilizer measurement circuit. The blue arrows show the circuit order for measuring an X-type stabilizer for both codes.

qubit ancillary states to ensure each faulty gate in the syndrome circuit could produce only one error on the data [20–22]. A second approach allows multiple errors to propagate to the data, but uses ancillary qubit measurements to inform the decoder of these errors [23–25]. The third approach notes that some multi-qubit errors can be tolerated as if they were single-qubit errors [11].

The surface code is considered a promising candidate for fault-tolerant quantum computing [26–28]. It is also a popular choice for implementing error correction on near-term small quantum devices [2, 11, 29, 30] due to its ability to restrict all stabilizer measurements as local operations. Fault-tolerant syndrome measurement with a bare ancillary qubit per check operator relies on a proper choice of circuit for implementing syndrome measurement, as illustrated in Fig.1b. This choice has been previously described as directing the hook errors away from the direction of the logical error [11], but when viewed from the perspective of the compass code the measurement circuits are determined by the underlying gauge operators.

The two-dimensional Bacon-Shor code has $L-1$ X stabilizers that correspond to a double column of Xs and the $L-1$ Z stabilizers that correspond to a double row of Zs. The logical X operators are $X^{\otimes L}$ acting on all qubits in the same column, and logical Z operators are $Z^{\otimes L}$ acting on all qubits in the same row. Bacon-Shor is a subsystem code and the extra degrees of freedom result in gauge operators acting trivially on the encoded information [14]. We use these gauge degrees of freedom to fault-tolerantly and directly measure each stabilizer using a single bare ancillary qubit.

The challenge of fault-tolerant $2L$-weight stabilizer measurement is that errors on the ancillary qubit can generate hook errors of weight $\lfloor (L-1)/2 \rfloor$ on the data. By measuring the stabilizers following the structure of the gauge operators, the hook errors are simply products of gauge operators and a single qubit error. Therefore, hook errors are equivalent to single qubit errors and $\lfloor d/2 \rfloor$-fault-tolerance is preserved for the code. Topologically one can consider the sequential product of gauge errors as a string with both ends attached to the same boundary and is therefore a trivial operator. This is in contrast to logical operators where the strings connect opposite boundaries [9].

For the X stabilizers, the circuit consists of preparing the ancillary qubits in $|+\rangle = X|+\rangle$ and then performing $2L$ controlled-not gates with each data qubit as the target and the ancillary qubit as the control, followed by measurement in the X basis. We order the controlled-not gates such that the target qubits come in pairs that follows the XX gauge operators. The stabilizer $S_{i,x} = \prod_{j=1,L} X_{j,i}X_{j,i+1}$, where $X_{j,i}X_{j,i+1}$ is the gauge operator on the qubits in row j and columns i and $i+1$, yields the sequence of controlled-nots $\prod_{j=1,L} \mathrm{CNOT}(a_i, d_{i,j})\mathrm{CNOT}(a_i, d_{i+1,j})$ where the target qubits d are paired by the gauge operator and controlled by the ancilla a. (Fig. 1c). A similar order holds for the Z stabilizers, where now the ancilla is prepared and measured in the Z basis and the controlled-nots target the ancilla qubits. This circuit has already been implemented experimentally in trapped ions and superconducting qubits for the $L = 2$ Bacon-Shor quantum error detection code [31, 32].

In addition to syndrome measurement, preparation of logical states is also an essential part of quantum error correction. For the surface code, to encode logical $|0\rangle$ we prepare all the data qubits in the physical $|0\rangle$ state, measure X type stabilizers L times and perform correction based on the syndrome. This procedure measures $(L^2-1)/2$ X stabilizers L times and requires $2L^2(L-1)$ two-qubit gates. For Bacon-Shor, to encode logical $|0\rangle$ we prepare L L-qubit GHZ states in the X basis along the rows without verification. Generating the L GHZ states only requires $L(L-1)$ two-qubit gates, significantly fewer gates than preparation by projecting onto the stabilizers. We note that this deterministic preparation is fault-tolerant for Bacon-Shor codes, since each row fails

independently and $\lceil L/2 \rceil$ rows must fail for the preparation to yield an incorrect logical measurement. Like the Bacon-Shor code itself, this preparation has no threshold and for fixed qubit error rate, there will be an optimal L for state preparation.

We now consider the smallest Bacon-Shor code on the 3×3 lattice. We need one ancillary qubit per stabilizer to perform fault-tolerant syndrome measurement of the [[9,1,3]] Bacon-Shor code, yielding a total of 13 qubits. We refer to this choice as Bacon-Shor-13 following the notation of Tomita and Svore where the [[9,1,3]] surface code with 8 ancilla is referred to as Surface-17 [11].

To compare the performance of Bacon-Shor-13 and Surface-17 we focus on simulating a circuit with 3 elements: logical state encoding, quantum error correction, and measurement of the individual data qubits. We refer to this circuit as the simple circuit. Using the measurement results, we determine the outcome of the logical circuit and the probability that the circuit fails.

To perform error correction using Surface-17 and Bacon-Shor-13, we designed a two-step lookup table decoders for both codes. The details of the Surface-17 decoder can be found at [2]. For any two-step decoder, in the first step if the syndrome shows no errors then no correction is performed; if the syndrome shows errors, then a second syndrome is measured and correction is applied based on the second syndrome. All simulations are performed using the stabilizer simulation program *CHP* [33] inside an importance sampling routine [2, 34]. State preparation of Bacon-Shor determinstically constructs the logical state, $|0\rangle_L = \bigotimes_{i=0}^{2} \frac{1}{\sqrt{2}}(|+++\rangle + |---\rangle)_{0+i,3+i,6+i}$ while Surface-17 requires 2 or 3 rounds of X stabilizer measurement due to the inherent projection noise of the measurements [2].

We consider two error models: a standard depolarizing error model and an ion trap inspired error model. We assume arbitrarily connected qubits for both cases, but for the ion trap error model the duration of two-qubit gates depends on ion distance [2]. Here we describe the error model in terms of Kraus operators.

Standard Error Model: The one- and two-qubit Kraus channels are of the form

$$\begin{aligned} E_1 &= \{\sqrt{1-p}I, \sqrt{\frac{p}{3}}X, \sqrt{\frac{p}{3}}Y, \sqrt{\frac{p}{3}}Z\}, \\ E_2 &= \{\sqrt{1-p}II, \sqrt{\frac{p}{15}}IX, \ldots, \sqrt{\frac{p}{15}}ZZ\}, \end{aligned} \tag{1}$$

where p is the error rate of the error channel. For each gate in the circuit, an element from the one-qubit (two-qubit) Pauli group is sampled and applied after the gate (before for measurements) to serve as an error.

Ion Trap Error Model: Quantum error correction circuits are constructed from Mølmer-Sørensen entangling gates, $\exp(-i(\theta/2)XX)$, and single qubit rotations, RX and RY [2, 35, 36]. The error model assumes that the main source of error comes from fluctuations in the control strength. The Kraus channels for the control errors

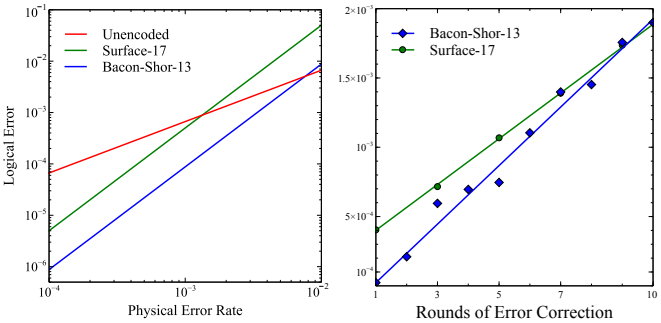

(a) One round of error correction

(b) Multiple rounds of error correction

FIG. 2: Comparison of Bacon-Shor-13 and Surface-17 in a simple circuit simulation. (a) With one round of error correction Bacon-Shor-13 shows a pseudothreshold of 0.9% and Surface-17 shows a pseudothreshold of 0.1%. The difference is mainly due to the difference in logical state preparation. (b) At a physical error rate of 10^{-3}, Surface-17 starts to outperform Bacon-Shor-13 in more than 9 rounds of error correction.

associated with these gates are

$$\begin{aligned} E_{XX} &= \{\sqrt{1-p_{XX}}II, \sqrt{p_{XX}}XX\}, \\ E_{RX} &= \{\sqrt{1-p_{RX}}I, \sqrt{p_{RX}}X\}, \\ E_{RY} &= \{\sqrt{1-p_{RY}}I, \sqrt{p_{RY}}Y\}, \end{aligned} \tag{2}$$

where in our simulation p_{XX} is the Mølmer-Sørensen control error rate and $P_{XX} = 10\,p_{RX} = 10\,p_{RY}$. The Mølmer-Sørensen gate couples ions through the collective ion motion and an error can occur due to heating of the motion during the gate. We can add a motional mode heating error with the Kraus channel

$$E_{heating} = \{\sqrt{1-p_h}II, \sqrt{p_h}XX\}, \tag{3}$$

where $p_h = \dot{\bar{n}}/2k \times t_{MS}$, where $\dot{\bar{n}}$ is the heating rate, k is the number of phase space loops of the motion during the gate, and t_{MS} is the duration of the corresponding entangling Mølmer-Sørensen gate. This error model follows Ref. [37].

During one and two-qubit gates, uncontrolled Stark shifts can also lead to a gate-induced dephasing error modeled with the single-qubit Kraus channel

$$E_{dephasing} = \{\sqrt{1-p_d}I, \sqrt{p_d}Z\}, \tag{4}$$

where $p_d = r_d \times t_g$, r_d is the dephasing rate and t_g is the time of the applied gate.

The results of the standard depolarizing error model are shown in Fig.2. The logical error of the simple circuit scales quadratically with the physical error rate showing that both protocols are 1-fault-tolerant as expected (Fig.2a). The higher logical error of Surface-17 is due primarily to the overhead of state preparation. When

Code	Prep	QEC	Measure	Total
Surface-17	2400-3600	4900-9800	100	7400-13500
Bacon-Shor-13	1670	4310-8620	100	6080-10390

TABLE I: Time required (in μs) to execute a simple circuit in an ion trap model (see [2] and Supplementary Material). The times can vary as the rounds of stabilizer measurements depends on the results of syndrome measurements.

multiple rounds of error correction are executed, Surface-17's advantage in error correction starts to dominate. As shown in Fig. 2b, Surface-17 starts to outperform Bacon-Shor-13 in a simple circuit with more than 9 rounds of error correction when the physical error rate is 10^{-3}. Each round of error correction allows for a logical gate and the performance of 9 rounds of error correction should be compared to the error of performing 9 physical gates $\approx 9 \times 10^{-3}$. The Bacon-Shor-13 logical error shows more variation around the trend line for odd rounds of error correction. We suspect this is due to the subsystem nature of the code but have not found a clear reason.

To simulate the performance of error-correcting codes in trapped-ion system we map the codes onto a linear ion chain and compile controlled-not gates from Mølmer-Sørensen gates [36, 38]. The linear chain can be split apart to allow measurement of ancillary qubits without affecting the data and then rejoined for further quantum operations Ref. [2]. Us- ing a simulated annealing algorithm, we searched for ion chain arrangements that minimized total time for quan- tum error correction or average two-qubit gate time (see Supplementary Material). In our ion trap error model gate error scales with two-qubit gate time and minimizing average two-qubit gate time minimizes the error due to ion heating and dephasing. Times required to execute the simple circuit when the ions are arranged to minimize the average two-qubit gate time are shown in TABLE I. Bacon-Shor-13 has shorter circuit execution time. These reported times are not fundamental and can be improved by changes in gate and measurement schemes [1, 39] but for all protocols, Bacon-Shor-13 will maintain the time advantage.

In Fig. 3 we present the results of comparing Bacon-Shor-13 and Surface-17 in a simple circuit with one round of error correction under the influence of different ion trap error sources. Here we assume the error rate for single-qubit gates and measurements is $\frac{1}{10}$ of two-qubit gates in order to match realistic error rates in experiments. All results are computed for an optimization of ion chain arrangement that minimizes average 2-qubit gate times for both codes independently.

From Fig. 3 we notice that for all error sources and strengths Bacon-Shor-13 outperforms Surface-17. For both codes, the simulated simple circuit would outperform a single two-qubit gate assuming only Mølmer-Sørensen control errors with rate below 10^{-3}. The heating rate and gate-induced dephasing error both raise the effective two-qubit error rate and this further separates the performance between Bacon-Shor-13 and Surface-17 for this circuit. These results indicate that a total two-qubit gate error rate of 10^{-3} should clearly demonstrate that an encoded circuit outperforms the unencoded circuit.

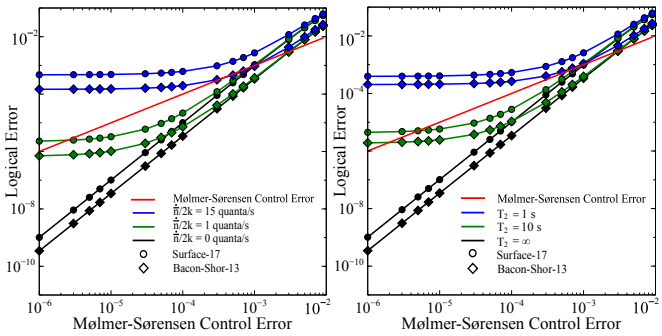

(a) Ion heating error (b) Spin dephasing error

FIG. 3: Comparison of Bacon-Shor-13 and Surface-17 with a simple circuit under the influence of an ion trap error model (see text). Logical error is plotted as a function of a control error in the Mølmer-Sørensen gate. Each plot includes an additional error due to ion heating ($\dot{n}$) or gate-induced dephasing (T_2) that depends on gate time.

In conclusion, we have found that for subsystem and subspace codes derived from the compass model the gauge operators prescribe a method for fault-tolerant stabilizer measurement. This yields the ability to fault-tolerantly measure large stabilizer operators with single ancillary qubits and provides insight into previous work on small surface codes. These results does require increasing qubit connectivity and becomes impractical for local architectures as the stabilizer size grows. We have also noted that for any size Bacon-Shor code state preparation can be performed in a deterministic fault tolerant manner compared to the project and error correct method commonly proposed for state preparation.

These general results have practical implications for near term quantum devices. Specifically we have shown that Bacon-Shor-13 outperforms Surface-17 in all measures for a simple circuit: time, logical error rate, and number of qubits. The key advantage of Bacon-Shor-13 over Surface-17 comes from its greatly simplified state preparation. In addition, the lower qubit count makes Bacon-Shor-13 a more immediate target for near-term quantum error correction in systems where non-nearest neighbor gates are possible, such as trapped ions. However as Surface-17 holds advantage over Bacon-Shor-13 in terms of error correction, multiple rounds of error correction will begin to favor Surface-17.

We note that the compass model code on an $L \times L$ lattice allows for a family of codes defined by how the gauge operators are fixed and the Bacon-Shor and rotated surface code are two extremes of this family. We

are currently studying this family of codes to determine what choice of gauges would yield a threshold, as the codes transition from Bacon-Shor to surface code [40].

We thank Dave Bacon, Andrew Cross, Cody Jones, and Colin Trout for useful discussions. This work was supported by the Office of the Director of National Intelligence - Intelligence Advanced Research Projects Activity through ARO contract W911NF-10-1-0231, the ARO MURI on Modular Quantum Systems W911NF-16-1-0349, the National Science Foundation grant PHY-1415461, and the Alexander von Humboldt Foundation.

Appendix A: Ion trap operation times

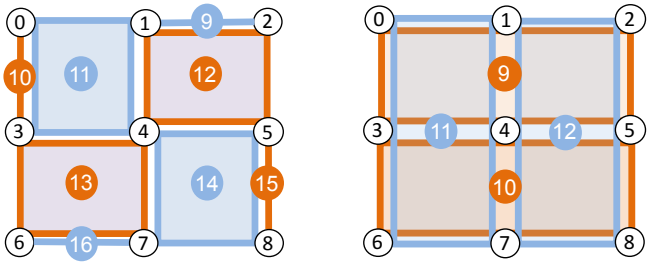

(a) Surface-17 (b) Bacon-Shor-13

FIG. 4: Qubit labeling for the [[9,1,3]] surface code and Bacon-Shor code. Data qubits, ancillary qubits for X type stabilizers, and ancillary qubits for Z type stabilizers are shown in black, blue, and orange circles, respectively.

Here we present some results on trap operation times for ion arrangements optimized according to different parameters. More details of the ion trap model and justification for the parameters are available in Ref. [2]. The optimization takes into account that although 2-qubit gates can occur between any pair of ions, the gate time will depend on the ion distance. It also assumes that before the ancillary qubits are measured they must be physically displaced from the data qubits. If the data qubits and ancillary qubits are separated in the chain, the number of joining and splitting steps is reduced at the cost of longer logical gate times. We note that neither limit is fundamental. It is possible to make 2-qubit gates where there is no time dependence on ion distance by adjusting laser power [39] and that ancillary qubits do not need to be separated when two ion species are used [1].

The optimization was done using a simulated annealing algorithm with an objective function adjusted for different optimization parameters, total time assuming two parallel gates (T) or average 2-qubit gate time (A), and different constraints, mixed (M) or separated (S) data and ancillary qubits. For each optimization label we calculate times for operations performed in both serial and parallel. Parallel operations allow for two simultaneous two-qubit gates exciting the independent x and y radial modes and fully parallel single-ion operations. We assume single-qubit gates, parallel measurement/state preparation, and shuttling between operation and measurement zones require 10 μs, 100 μs, and 100 μs, respectively. The shuttling operation includes the time to split and join ion chains. The results in the paper are for the MA optimization, which minimizes error for the error correction step. In Ref. [2], the reported results for Surface-17 are for MT.

Code	Opt.	Logic	Shuttle	Meas.	Total
Surface-17	SA	7240 (3920)	200	100	7950 (4220)
	MA	2300 (1170)	1800	800	4900 (3770)
	MT	4300 (2320)	700	300	5300 (3320)
Bacon-Shor-13	SA	5580 (3270)	200	100	5880 (3570)
	MA	2910 (1490)	1000	400	4310 (2890)
	MT	3580 (1860)	400	100	4080 (2360)

TABLE III: Trap operation times (in μs) for one round of error correction calculated according to ion arrangements optimized for an array of parameters (see text). All values are reported in μs and the numbers in parentheses refer to the gate time when two 2-qubit operations are performed in parallel.

Code	Opt.	Prep Time
Surface-17	SA	7880-11820 (4460-6690)
	MA	2400-3600 (1200-1800)
	MT	3800-5700 (2100-3150)
Bacon-Shor-13	SA	670 (450)
	MA	1670 (1040)
	MT	1480 (970)

TABLE IV: Trap operation times (in μs) for logical state preparation calculated according to ion arrangements optimized for an array of parameters (see text). The time for Surface-17 can vary as it is a probabilistic circuit of syndrome extraction.

Code	Opt.	Ion Arrangement
Surface-17	SA	0 2 6 8 1 4 3 7 5 **11** **12** **10** **15** **13** **14** **9** **16**
	MA	2 **9** 1 **12** 5 **15** 8 **14** 4 **11** 0 **10** 3 **13** 7 **16** 6
	MT	**10** **15** **9** 5 0 1 **11** **12** **14** 7 4 3 8 2 6 **13** **16**
Bacon-Shor-13	SA	0 2 6 8 1 3 7 5 4 **11** **10** **12** **9**
	MA	8 2 **12** 1 5 **9** 4 **10** 7 3 **11** 0 6
	MT	2 1 5 4 **9** **12** **10** **11** 7 3 0 8 6

TABLE II: Ion arrangements optimized for an array of parameters (see text). Numbers in bold face represent ancillary qubits.

[1] A. Bermudez, X. Xu, R. Nigmatullin, J. O'Gorman, V. Negnevitsky, P. Schindler, T. Monz, U. G. Poschinger, C. Hempel, J. Home, et al., Phys. Rev. X **7**, 041061 (2017).

[2] C. J. Trout, M. Li, M. Gutiérrez, Y. Wu, S.-T. Wang, L. Duan, and K. R. Brown, New Journal of Physics **20**, 043038 (2018).

[3] T. E. O'Brien, B. Tarasinski, and L. DiCarlo, npj Quantum Inf. **3**, 39 (2017).

[4] J. Kelly, R. Barends, A. Fowler, A. Megrant, E. Jeffrey, T. White, D. Sank, J. Mutus, B. Campbell, Y. Chen, et al., Nature **519**, 66 (2015).

[5] T. H. Taminiau, J. Cramer, T. van der Sar, V. V. Dobrovitski, and R. Hanson, Nat. Nanotechnol. **9**, 171 (2014).

[6] D. G. Cory, M. D. Price, W. Maas, E. Knill, R. Laflamme, W. H. Zurek, T. F. Havel, and S. S. Somaroo, Phys. Rev. Lett. **81**, 2152 (1998).

[7] J. Chiaverini, D. Leibfried, T. Schaetz, M. D. Barrett, R. Blakestad, J. Britton, W. M. Itano, J. D. Jost, E. Knill, C. Langer, et al., Nature **432**, 602 (2004).

[8] P. Schindler, J. T. Barreiro, T. Monz, V. Nebendahl, D. Nigg, M. Chwalla, M. Hennrich, and R. Blatt, Science **332**, 1059 (2011).

[9] S. B. Bravyi and A. Y. Kitaev, arXiv:quant-ph/9811052 (2011).

[10] H. Bombin and M. A. Martin-Delgado, Phys. Rev. A **76**, 012305 (2007).

[11] Y. Tomita and K. M. Svore, Phys. Rev. A **90**, 062320 (2014).

[12] D. Bacon, Phys. Rev. A **73**, 012340 (2006).

[13] P. W. Shor, Phys. Rev. A **52**, R2493 (1995).

[14] P. Aliferis and A. W. Cross, Phys. Rev. Lett. **98**, 220502 (2007).

[15] J. Napp and J. Preskill, Quantum Info. Comput. **13**, 490 (2013).

[16] T. J. Yoder, arXiv preprint arXiv:1705.01686 (2017).

[17] Z. Nussinov and J. Van Den Brink, Rev. Mod. Phys. **87**, 1 (2015).

[18] A. Kitaev, Annals of Physics **321**, 2 (2006).

[19] E. Dennis, A. Kitaev, A. Landahl, and J. Preskill, Journal of Mathematical Physics **43**, 4452 (2002).

[20] P. W. Shor (IEEE Computer Society Press, 1996), FOCS '96, pp. 56–65.

[21] A. M. Steane, Phys. Rev. Lett. **78**, 2252 (1997).

[22] E. Knill, Nature **434**, 39 (2005).

[23] D. P. DiVincenzo and P. Aliferis, Physical review letters **98**, 020501 (2007).

[24] T. J. Yoder and I. H. Kim, Quantum **1**, 2 (2017).

[25] R. Chao and B. W. Reichardt, Physical review letters **121**, 050502 (2018).

[26] R. Raussendorf and J. Harrington, Phys. Rev. Lett. **98**, 190504 (2007).

[27] A. G. Fowler, A. M. Stephens, and P. Groszkowski, Phys. Rev. A **80**, 052312 (2009).

[28] C. Horsman, A. G. Fowler, S. Devitt, and R. Van Meter, New J. Phys. **14**, 123011 (2012).

[29] A. G. Fowler, M. Mariantoni, J. M. Martinis, and A. N. Cleland, Phys. Rev. A **86**, 032324 (2012).

[30] R. Versluis, S. Poletto, N. Khammassi, B. Tarasinski, N. Haider, D. Michalak, A. Bruno, K. Bertels, and L. DiCarlo, Phys. Rev. Appl. **8**, 034021 (2017).

[31] N. M. Linke, M. Gutierrez, K. A. Landsman, C. Figgatt, S. Debnath, K. R. Brown, and C. Monroe, Sci. Adv. **3**, e1701074 (2017).

[32] M. Takita, A. W. Cross, A. D. Córcoles, J. M. Chow, and J. M. Gambetta, Phys. Rev. Lett. **119**, 180501 (2017).

[33] S. Aaronson and D. Gottesman, Phys. Rev. A **70**, 052328 (2004).

[34] M. Li, M. Gutiérrez, S. E. David, A. Hernandez, and K. R. Brown, Phys. Rev. A **96**, 032341 (2017).

[35] A. Sørensen and K. Mølmer, Phys. Rev. Lett. **82**, 1971 (1999).

[36] D. Maslov, New J. Phys. **19**, 023035 (2017).

[37] C. J. Ballance, T. P. Harty, N. M. Linke, M. A. Sepiol, and D. M. Lucas, Phys. Rev. Lett. **117**, 060504 (2016).

[38] K. Mølmer and A. Sørensen, Phys. Rev. Lett. **82**, 1835 (1999).

[39] P. H. Leung, K. A. Landsman, C. Figgatt, N. M. Linke, C. Monroe, and K. R. Brown, Phys. Rev. Lett. **120**, 020501 (2018).

[40] M. Li, D. Miller, M. Newman, Y. Wu, and K. R. Brown, arXiv preprint arXiv:1809.01193 (2018).